Volume 1 | Number 1 | Jan 2013 | Pages 1–100

ChemComm

Chemical Communications
www.rsc.org/chemcomm

ROYAL SOCIETY
OF CHEMISTRY

This is an *Accepted Manuscript*, which has been through the Royal Society of Chemistry peer review process and has been accepted for publication.

Accepted Manuscripts are published online shortly after acceptance, before technical editing, formatting and proof reading. Using this free service, authors can make their results available to the community, in citable form, before we publish the edited article. We will replace this *Accepted Manuscript* with the edited and formatted *Advance Article* as soon as it is available.

You can find more information about *Accepted Manuscripts* in the **Information for Authors**.

Please note that technical editing may introduce minor changes to the text and/or graphics, which may alter content. The journal's standard **Terms & Conditions** and the **Ethical guidelines** still apply. In no event shall the Royal Society of Chemistry be held responsible for any errors or omissions in this *Accepted Manuscript* or any consequences arising from the use of any information it contains.

ROYAL SOCIETY
OF CHEMISTRY

www.rsc.org/chemcomm

Journal Name

COMMUNICATION

Electrochemically-driven drug metabolism via CYP1A2/UGT1A10 bienzymes confined in graphene nano-cage

Jusheng Lu, Yuanjian Zhang, Henan Li, Jiachao Yu and Songqin Liu*

A graphene nano-cage with regulatable space for assembly of cytochrome P450 1A2/UDP-glucuronosyltransferase 1A10 bienzyme complexes has been constructed via click reaction, which is successfully used to study the drug sequential metabolism by an electrochemically-driven way.

The metabolic activities of organisms in the substrate of a biological reaction system are highly coordinated by the formation of supramolecular complexes of sequential metabolic enzymes.[1] The enzyme complexes make enzymes cannot freely diffuse within the cytosols, allowing the direct passage of a product from one enzymatic reaction to a consecutive enzyme in a metabolic pathway.[2] Moreover, the enzyme complexes limit the intermediates diffusing into the surrounding milieu, thus dramatically increasing the workload of the enzymes involved, facilitating fast turnover of labile or toxic intermediates, and preventing undesired crosstalk between different metabolic pathways.[3] Inspired by natural enzyme complexes, construction of artificial enzyme complexes and spatial organization of multiple enzymes with appropriate spacing could be an important approach to unravel the mechanisms of consecutive enzymatic reactions. Fu et al. organized discrete glucose oxidase/ horseradish peroxidase enzyme pairs on specific DNA origami tiles with controlled inter-enzyme spacing and position, and found the activity of the as-prepared enzyme complexes was higher than the free enzyme mixture.[4] Liu et al. reported the conjugation of enzymes with synergic or complementary functions to form a nanocomplex, which exhibited an enhanced stability when compared with free enzymes.[5]

In the present work, motivated by the great potential of the controllable mutli-enzyme complex formation in the biosynthesis and target cascade metabolism, we prepare a nano-cage for controllable assembly of enzymes. In which, graphene, a two-dimensional aromatic monolayer composed of sp^2-bonded carbon atoms with high specific surface area, electrical conductivity and superlative mechanical strength,[6] is utilized as a framework of the nano-cage, phase I cytochrome P450 1A2 (CYP1A2) enzyme and phase II UDP-glucuronosyltransferase 1A10 (UGT1A10) enzyme, as model enzymes, are respectively assembled in the bottom and top layers of the graphene nano-cage on the surface of glassy carbon electrode (GCE) to form bienzyme complexes (Scheme 1). Driven by an electrochemical way, the enzymatic activity of the artificial bienzyme complexes to warfarin sequential metabolism is successfully regulated by adjusting the interval distance of the nano-cage, i.e. adjusting the inter-enzyme spacing and spatial positions of the two enzymes. Such interesting enzyme complexes confined in the graphene nano-cage would offer a unique platform to investigate the process of drug metabolism in vitro.

In the construction process of artificial bienzyme complexes in graphene nano-cage, to improve the dispersion and biocompatibility, graphene was firstly modified with chitosan from graphene oxide by a chemical reduction to form a graphene-chitosan (GR/CS) nanocomposite, which is a monolayer nanosheet (Fig. S1†). The GR/CS nanosheet was then deposited on a GCE and followed by assembling CYP1A2 and α-amino-ω-azido poly (ethylene glycol) (NH$_2$-PEG-N$_3$) via glutaraldehyde-based cross-linking, forming GCE/GR/CS (CYP1A2)-PEG-N$_3$ (**1**). Meanwhile, UGT1A10 and α-amino-ω-

alkynyl poly (ethylene glycol) (NH$_2$-PEG-C≡CH) were cross-linked to another free GR/CS nanosheet, forming GR/CS(UGT1A10)-PEG-C≡CH (**2**). Finally, **2** was cross-linked onto **1** via a click reaction catalyzed by copper (I) ions,[7] forming bienzyme complexes in graphene nano-cage on the surface of GCE (**3**), which could be proved by the FT-IR spectra (Fig. S2†). The AFM images also show that the interlayer distance of the nano-cage can be manipulated simply by varying the chain length of PEG linkage (Fig. S3†). The amount of CYP1A2 and UGT1A10 assembled on the bottom or upper layers of graphene nanosheets, determined by the Bradford assay (Fig. S4†),[8] is ca. 0.51 and 0.42 μmol m^{-2} GCE, respectively.
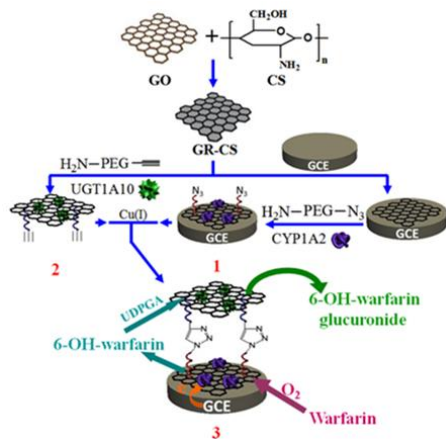
Scheme 1 Construction process of artificial bienzyme complexes in the graphene nano-cage

As a proof of the concept, we studied the activity of CYP1A2 and UGT1A10 assembled in the graphene nano-cage for the sequential metabolism of warfarin. Generally, in human liver, warfarin is first mainly converted into 6-hydroxywarfarin (6-OH-WAR) catalysed by phase I enzyme CYP1A2 with NADPH as electron donor, and further reacts with UDP glucuronic acid (UDPGA) under phase II enzyme UGT1A10 to form glucuronide metabolite (Scheme S1†).[9] In our assemblies, the sequential metabolism of warfarin can be electrochemically-driven by bienzyme complexes in the graphene nano-cage under the aerobic conditions with GCE for electron donation. The related electrochemical responses of different assembly systems are shown in Fig. 1. In an anaerobic 0.1 M PBS (pH7.4), for the enzymes in graphene nano-cage, a pair of stable and well-defined redox peaks with similar height is observed at -0.539 and -0.485 V (vs SCE), respectively (curve a, Fig. 1A), while no redox peaks appear for the GCE/GR/CS(UGT1A10), GCE/GR or GCE/GR/CS (curve c-e, Fig. 1B). It indicates that the response is attributed to the quasi-reversible direct electron transfer between the heme electroactive site of CYP1A2 and the GCE, i.e., CYP1A2 is electrochemically active and has good electrochemical stability in the nano-cage (Fig. S5†), while UGT1A10 has not electrochemical activity. With an increase of scan rate, the anodic and cathodic peak potentials exhibit a small shift and the peak currents increase linearly, characteristic of a surface-controlled process.[10] Based on Laviron's method,[11] the

electron transfer rate constant (K_s) of CYP1A2 on the modified GCE is calculated to be 5.37 s^{-1} at a scan rate of 0.1 V s^{-1} (Fig. S6†). As a control, when CYP1A2 and UGT1A10 enzymes are directly assembled on the bare GCE (GCE/CYP1A2&UGT1A10) or GR modified GCE (GCE/GR/CYP1A2&UGT1A10), rather than on the GCE/GR/CS, only very weak redox peaks are observed (curve a and b, Fig. 1B), due to the partial denaturation of CYP1A2 on the GCE[12] and little assembly amount of CYP1A2 on the GCE. It further illustrates the biocompatibility of GR/CS with rich functional groups. Furthermore, it is worthy of noting that the exact assembly position of enzymes affect the electron transfer between the enzyme and the GCE. When UGT1A10 is assembled on the bottom layer and CYP1A2 on the top layer. Although the redox peaks of CYP1A2 also appear, the peak currents decrease considerably in comparison with that before exchange of the enzyme position (curve b, Fig. 1A). These results indicate when immobilized on the bottom layer of graphene nano-cage, the electrochemically inert UGT1A10 and the increase of the distance between the active center of CYP1A2 and GCE profoundly affect the electron transfer between CYP1A2 and GCE. Therefore, simply by assembling enzymes on the graphene separately before the final cross-linking, the position of the enzymes in the nano-cage can be controlled, making the proposed artificial enzyme complexes more flexible for the fundamental studies of cascade multi-enzymes in vitro.
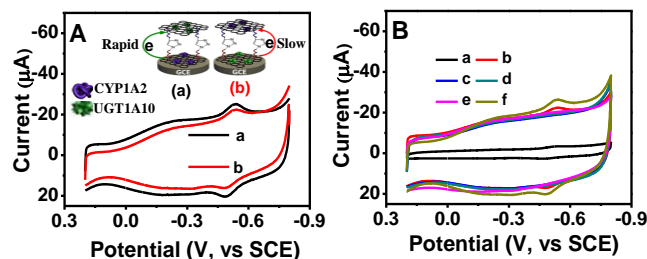

Fig. 1 Electrochemical responses of different assembly systems. (A) CVs of the graphene nano-cage modified GCE with CYP1A2 in the bottom layer (a) or upper layer (b); (B) CVs of GCE/CYP1A2&UGT1A10 (a), GCE/GR/CYP1A2&UGT1A10 (b), GCE/GR/CS/UGT1A10 (c), GCE/GR/CS (d), GCE/GR (e) and GCE/GR/CS/CYP1A2 (f). Electrolyte solution: anaerobic 0.1 M PBS (pH 7.4); Scan rate: 0.1 V s^{-1}.

Under the aerobic condition, the addition of warfarin into the electrolyte leads to the increase of the reduction peak current of CYP1A2 in the nano-cage. The reduction current increases with the concentration of warfarin (see steady state CVs in Fig. 2A). However, as a control, only a little increase of the reduction current is observed for GCE/GR/CYP1A2&UGT1A10 after addition of warfarin, which is much smaller than that of CYP1A2 in the nano-cage (Fig. S7†), indicating the successful electrochemically-driven catalytic behaviour of the bienzyme complexes in the nano-cage for warfarin cascade metabolism. Fig. 2B shows the electrocatalytic kinetic responses of the enzymes to warfarin in the graphene nano-cages linked by PEGs with different chain lengths as a function of the warfarin concentration. Fitting the results with the Michaelis-Menten

model,[13] the calculated apparent Michaelis constant K_m decreases exponentially with increasing the chain length of PEG linkage, and finally reaches a minimum value when the chain length of PEG is 2000/2000 (Fig. 2C). Further increase the chain length of PEG, the K_m increases on the contrary. It is because that, too short chain PEG linkage leads to small confined space of the graphene nano-cage, resulting in the conformational distortion of the entrapped enzymes. While too large long chain PEG linkage results in the longer inter-enzyme spacing of the nano-cage, easily leading to the diffusion of substrates and intermediates into the surrounding milieu. Similarly, as shown in Fig. 2 C and D, when the chain length of PEG increases, the maximum current I_{max}, catalytic rate constant k_{cat} and catalytic efficiency k_{cat}/K_m increase to maximum and then decrease. Furthermore, the optimized K_m (3.23 μM) here is far less than that of free CYP1A2 in the solution (1.6 mM),[14] and the corresponding I_{max} (12.04 μA), k_{cat} (6.23 s^{-1}), and k_{cat}/K_m (1.94 μM^{-1}s^{-1}) are far more than those in the relevant literatures,[15] indicating the enzymes spatially confined in the proposed graphene nano-cage has a much superior biocatalytic activity and excellent catalytic efficiency to warfarin in comparison with those in the free state, which is similar to those studied in previous reports.[16] This typical confinement effect of enzyme affinity and catalytic properties evidently demonstrates that control of the chain length of PEG between the upper and lower layers of nano-cage can effectively regulate the kinetics of enzymes in metabolism of substrates.
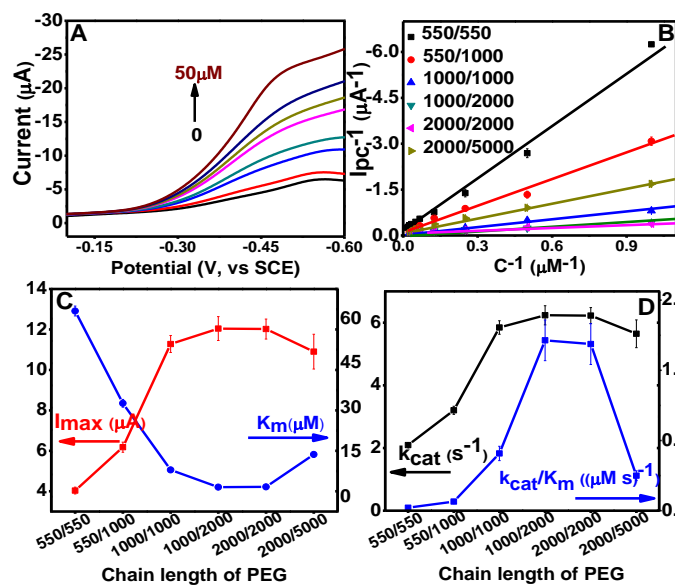

Fig. 2 Kinetic mechanism of enzymes in the graphene nano-cage. (A) Influence of warfarin concentration (0, 2, 4, 8, 15, 20, 40, 50 μM) on rotating disk voltammograms (1000 rpm) of enzymes in graphene nano-cage; (B) Lineweaver-Burke plots of catalytic current of enzymes in the graphene nano-cages with different PEG chain length linkage and the concentration of warfarin; (C) Influence of PEG chain length on the value of K_m and I_{max}; (D) Influence of PEG chain length on the value of k_{cat} and k_{cat}/K_m. Electrolyte solution: aerobic 0.1 M PBS (pH 7.4); Scan rate: 0.1 V s^{-1}.

As shown in Fig. S8†, with the increase of the amount of ciprofloxacin, an inhibitor of CYP1A2 for the high affinity toward CYP1A2,[17] the catalytic peak current of CYP1A2 continuously decreases and reaches a relatively stable value as the concentration is higher than 100 μM. The IC$_{50}$ value, a concentration of inhibitor producing 50% inhibition, is determined as 36.6 μM, which is lower than those reported in the literature ranging from 135 to 300 μM,[18] further indicating the enzymes spatially confined in the graphene nano-cage retain their bioactivity.

To confirm the electrochemically-driven cascade metabolic process of warfarin, the enzymes in graphene nano-cage modified GCE was electrolyzed at -0.54 V (vs SCE) in the presence of 100 μM warfarin under aerobic conditions for 1 h. After that, the warfarin metabolites were analysed by LC-MS/MS. As a control, the warfarin metabolites in graphene nano-cage only containing CYP1A2 were also analysed. It is found before the electrolysis, the liquid chromatogram of pure warfarin shows a sharp peak at 7.577 min (Fig. S9A†). At the CYP1A2-graphene nano-cage modified GCE, after electrolysis, one more peak at 6.812 min is observed (Fig. S9B†).When the electrolysis is carried out at graphene nano-cage containing both CYP1A2 and UGT1A10 bienzymes, a new peak at 5.725 min appears (Fig. S9C†). The cascade metabolic process of warfarin was also confirmed by electrospray ionization-mass spectrometry (ESI-MS). Before the electrolysis, only the peaks at 251.2, 163.1, 147.0 m/z corresponding to molecular ion of warfarin and its fragment ions were observed (Fig. S9D†). After phase I enzyme warfarin metabolism by CYP1A2, the peaks of 325.4 and 267.3 m/z appear (Fig. S9E†), which illustrates the formation of phase I metabolite, 6-OH-WAR. When the bienzyme complexes were assembled in graphene nano-cage, and further used for cascade metabolism of warfarin, three new peaks at 501.4, 443.2 and 355.1 m/z are observed (Fig. S9F†), which are attributed to the 6-OH-WAR glucuronide ion and its fragment ions. All these results demonstrate that the successful construction of bienzyme complexes in the graphene nano-cage to undertake similar drug cascade metabolic process in vivo by an electrochemically-driven way. It holds great potential for mimicking the multi-enzymes metabolism in vivo, and intervening metabolic processes.

For verify the importance and indispensability of the graphene nano-cage in construction of the bienzyme complexes, as a control, the metabolism of warfarin catalysed by a specific assembly system of GCE/GR/CS/CYP1A2-PEG-UGT1A10, UGT1A10 was covalent anchored at the PEG chain without the upper layer of GR/CS, was studied by the electrochemically driven way. The analytical results of LC-MS/MS show that only phase I metabolite 6-hydroxywarfarin appears, while no phase II metabolite 6-hydroxywarfarin glucuronide in the electrolyte solution was detected. The possible reason is that, the substrate warfarin is firstly catalysed by CYP1A2 to form an intermediate 6-hydroxywarfarin. However, because of the relatively open environment of the specific assembly system, the intermediate cannot effectively reach the active sites of UGT1A10, but mostly diffuse into the surrounding solution, resulting in negligible phase

II metabolite. It further illustrates the bienzyme complexes spatially confined graphene nano-cage can limit the intermediate diffusing into the surrounding milieu, thus ensuring the formation of the substrate channeling of warfarin.

In summary, a novel interlayer-distance controllable graphene nano-cage for constructing enzyme complexes by respective assembling of phase I CYP1A2 and phase II UGT1A10 in the bottom and top layer of the nano-cage has been successfully fabricated. The immobilized CYP1A2 on the bottom layer of graphene nano-cage remained bioactivity to catalyse the metabolism of warfarin via an electrochemically-driven way. When phase II enzyme UGT1A10 is assembled further on the upper layer of the nano-cage, it can capture the intermediate by phase I enzyme CYP1A2, carrying out phase II enzyme metabolism, thus ensuring the formation of the substrate channeling of warfarin. Such metabolic pathway has the same function like that in vivo and the metabolic efficiency of the bienzyme complexes is significantly improved. Simultaneously, the enzymatic activity to warfarin cascade metabolism can be effectively regulated by changing the interlayer spacing of the graphene nano-cage, i.e. the chain length of PEG linkage between the upper and bottom layer of the nano-cage; the electron transfer properties of enzymes can also be manipulated by assembling enzymes in the specific positions of the nano-cage. Such interesting graphene nano-cage containing multiple enzymes can offer us a promising platform for studying the mechanisms of enzyme complexes formation and the function of enzyme complexes in metabolic process in vitro.

Notes and references

Jiangsu Province Hi-Tech Key Laboratory for Bio-medical Research, School of Chemistry and Chemical Engineering, Southeast University, Nanjing 211189, China. *E-mail: liusq@seu.edu.cn.

1 (a) S. Schoffelen and J. C. M. van Hest, *Soft Matter.*, 2012, **8**, 1736; (b) O. I. Wilner, Y. Weizmann, R. Gill; O. Lioubashevski, R. Freeman and I. Willner, *Nat. Nanotechnol.,* 2009, **4**, 249; (c) P. A. Srere, *Trends Biochem. Sci.,* 1985, **10**, 109; (d) C. Lindbladh, R. D. Brodeur, G. Lilius, L. Bulow, K. Mosbach and P. A. Srere, *Biochemistry,* 1994, **33**, 11684.

2 Y. H. P. Zhang, *Biotechnol. Adv.*, 2011, **29**, 715.

3 (a) R. Matsumoto, M. Kakuta, T. Sugiyama, Y. Goto, H. Sakai, Y. Tokita, T. Hatazawa, S. Tsujimura, O. Shirai and K. Kano, *Phys. Chem. Chem. Phys.,* 2010, **12**, 13904; (b) S. F. M. Van Dongen, M. Nallani, J. J. L. M. Cornelissen, R. J. M. Nolte and J. C. M. van Hest, *Chem. Eur. J.,* 2009, **15**, 1107; (c) C. M. Niemeyer, J. Koehler and C. Wuerdemann, *Chembiochem,* 2002, **3**, 242; (d) H. P. Fierobe, E. A. Bayer, C. Tardif, M. Czjzek, A. Mechaly, A. Belaich, R. Lamed, Y. Shoham and J. P. Belaich, *J. Biol. Chem.,* 2002, **277**, 49621; (e) B. L. Møller,. *Science,* 2010, **330**, 1328; (f) B. S. J. Winkel, *Annu. Rev. Plant Biol.*, 2004, **55**, 85; (g) C. Kristensen, M. Morant, C. E. Olsen, C. T. Ekstrom, D. W. Galbraith, B. L. Moller and S. Bak, *Proc. Natl. Acad. Sci. U S A,* 2005, **102**, 1779.

4 J. L. Fu, M. H. Liu, Y. Liu, N. W. Woodbury and H. Yan, *J. Am. Chem. Soc.,* 2012, **134**, 5516.

5 Y. Liu, J. J. Du, M. Yan, M. Y. Lau, J. Hu, O. O. Yang, S. Liang, W. Wei, H. Wang, J. M. Li, X. Y. Zhu, L. Q. Shi, W. Chen, C. Ji and Y. F. Lu, *Nat. Nanotech.,* 2013, **8**, 187.

6 (a) S. Stankovich, D. A. Dikin, G. H. B. Dommett, K. M. Kohlhaas, E. J. Zimney, E. A. Stach, R. D. Piner, S. T. Nguyen and R. S. Ruoff, *Nature,* 2006, **442**, 282; (b) C. N. R. Rao, A. K. Sood, K. S. Subrahmanyam and A. Govindaraj, *Angew. Chem. Int. Ed.,* 2009, **48**, 7752; (c) Z. S. Wu, K. Parvez, X. L. Feng and K. Müllen, *Nat. Commun.,* 2013, **4**, 2487; (d) I. V. Lightcap, T. H. Kosel and P. V. Kamat, *Nano Lett.,* 2010, **10**, 577-583; (e) A. K. Geim and K. S. Novoselov, *Nat. Mater.,* 2007, **6**, 183; (f) C. G. Lee, X. D. Wei, J. W. Kysar and J. Hone, *Science,* 2008, **321**, 385; (g) X. Q. Liu, F. Wang, R. Aizen and I. Willner, *J. Am. Chem. Soc.,* 2013, **135**, 11832; (h) X. Wang, L. Zhi and K. Müllen, *Nano Lett.,* 2008, **8**, 323; (i) Q. Zeng, J. S. Cheng, L. H. Tang, X. F. Liu, Y. Z. Liu, J. H. Li and J. H. Jiang, *Adv. Funct. Mater.,* 2010, **20**, 3366.

7 H. C. Kolb, M. G. Finn and K. B. Sharpless, *Angew. Chem. Int. Ed.,* 2001, **40**, 2004.

8 M. M. Bradford, *Anal. Biochem.,* 1976, **72**, 248.

9 (a) L. Lesko, *Clin. Pharmacol. Ther.,* 2008, **84**, 301; (b) A. Zielinska, C. F. Lichti, S. Bratton, N. C. Mitchell, A. Gallus-Zawada, V. H. Le, M. Finel, G. P. Miller, A. Radominska-Pandya and J. H. Moran, *J. Pharmacol. Exp. Ther.,* 2008, **324**, 139.

10 J. C. Myland and K. B. Oldham, *Electrochem. Commun.,* 2005, **7**, 282.

11 E. J. Laviron, *J. Electroanal. Chem.,* 1979, **101**, 19.

12 V. V. Shumyantseva, S. Carrara, V. Bavastrello, D. J. Riley, T. V. Bulko, K. G. Skryabin, A. I. Archakov and C. Nicolini, *Biosens. Bioelectron.,* 2005, **21**, 217.

13 C. Malitesta, F. Palmisano, L. Torsi and P. G. Zambonin, *Anal. Chem.,* 1990, **62**, 2735.

14 Z. Zhang, M. J. Fasco, Z. Huang, F. P. Guengerich and L. S. Kaminsky, *Drug Metab. Dispos.,* 1995, **23**, 1339.

15 (a) C. M. Mosher, M. A. Hummel, T. S. Tracy and A. E. Rettie, *Biochemistry,* 2008, **47**, 11725; (b) F. Jung, K. J. Griffin, W. Song, T. H. Richardson, M. Yang and E. F. Johnson, *Biochemistry,* 1998, **37**, 16270.

16 (a) S. J. Li, C. Wang, Z. Q. Wu, J. J. Xu, X. H. Xia and H. Y. Chen, *Chem. Eur. J.* 2010, **16**, 10186; (b) C. Wang, D. K. Ye, Y. Y. Wang, T. Lu and X. H. Xia, *Lab. Chip* 2010, **10**, 639; (c) Z. Q. Wu, W. Z. Jia, K. Wang, J. J. Xu, H. Y. Chen and X. H Xia, Anal. Chem. 2012, **84**, 10586.

17 H. Stass and D. Kubitza, *Clin. Infect. Dis.,* 2001, **32**, S47.

18 (a) M. J. Karjalainen, P. J. Neuvonen and J. T. Backman, *Basic Clin. Pharmacol. Toxicol.,* 2008, **103**, 157; (b) L. Zhang, M. J. Wei and C. Y. Zhao, *Acta Pharmacol. Sin.,* 2008, **29**, 1507.